Comparison of Switching Principles in Microfluidic Bus Networks

Medina Hamidović*
Institute for Communications Engineering and RF-Systems
Johannes Kepler University Linz
Linz, Austria
medina.hamidovic@jku.at

Werner Haselmayr
Institute for Communications Engineering and RF-Systems
Johannes Kepler University Linz
Linz, Austria
werner.haselmayr@jku.at

Andreas Grimmer
Institute for Integrated Circuits
Johannes Kepler University Linz
Linz, Austria
andreas.grimmer@jku.at

Robert Wille
Institute for Integrated Circuits
Johannes Kepler University Linz
Linz, Austria
robert.wille@jku.at

Andreas Springer
Institute for Communications Engineering and RF-Systems
Johannes Kepler University Linz
Linz, Austria
andreas.springer@jku.at

ABSTRACT

In this work, we investigate passive droplet routing in microfluidic bus networks as a promising approach for realizing programmable and flexible microfluidic devices. Two main concepts for passive droplet routing have been established in the past: switching by distance and switching by size. In this work, we deliver a unified analysis and comparison of both methods in terms of network size and achievable throughput. We complete the analysis by identifying the key limiting parameters for both metrics and providing some application specific design guidelines.

CCS CONCEPTS

• **Networks**; • **Hardware** → *Biology-related information processing*;

KEYWORDS

Droplet-based microfluidics, microfluidic bus network, passive droplet control

ACM Reference Format:
Medina Hamidović, Werner Haselmayr, Andreas Grimmer, Robert Wille, and Andreas Springer. 2018. Comparison of Switching Principles in Microfluidic Bus Networks. In *NANOCOM '18: NANOCOM '18: ACM The Fifth Annual International Conference on Nanoscale Computing and Communication, September 5–7, 2018, Reykjavik, Iceland*. ACM, New York, NY, USA, 6 pages. https://doi.org/10.1145/3233188.3233206

1 INTRODUCTION

Labs-on-Chip (LoCs) are microfluidic systems which aim to miniaturize, integrate and automate several laboratory functions on a single microfluidic chip [10]. Droplet-based microfluidic systems are a promising platform for the realization of LoCs [11]. In such systems small volumes of fluids, so-called droplets, flow in closed microchannels inside an immiscible carrier fluid. The droplets contain biological or chemical samples that are manipulated and analyzed on the chip. Due to the small volume of the droplets, high reaction rates and small consumption of reagents can be achieved. Moreover, the immiscibility between the carrier fluid and the droplets minimizes contamination and secondary effects from unwanted biochemical reactions. Hence, droplet-based microfluidics is beneficial for various applications, e.g., for DNA or protein synthesis [10].
In order to perform specific manipulations and analysis on the LoC it is crucial to control the path of the droplet throughout the chip. The droplets can be controlled actively or passively. Active control requires microvalves or externally applied electric forces, magnetic fields or surface acoustic waves [10]. Although these techniques provide precise droplet control, they suffer from complex and costly fabrication as well as biocompatibility for some biochemical entities. Passive droplet control exploits only hydrodynamic principles and, thus, can be fabricated at low cost and offer a higher degree of chemical compatibility. For these systems, channel geometries and applied hydrodynamic forces are critical design parameters.
Recently, microfluidic networks [3, 5, 8, 9] as well as corresponding design methods [6, 7] have been introduced, which aim at realizing programmable and flexible LoC devices using passive droplet control. In particular, the goal is to dynamically assign the droplets' path through a microfluidic network in order to perform specific manipulations and analyses. The key elements in such microfluidic networks are microfluidic switches (μfSwitches), which are able to control the path of the droplet. This is accomplished by sending a so-called *header* droplet in front of the droplet containing the biological/chemical samples, so-called *payload* droplet. Header droplets are only used for signaling and contain no sample. The target location of the payload droplet can be either encoded in the distance between payload and header droplet [5], so-called *droplet*

*Corresponding author.

NANOCOM '18, September 5–7, 2018, Reykjavik, Iceland

ACM ISBN 978-1-4503-5711-1/18/09…$15.00
https://doi.org/10.1145/3233188.3233206

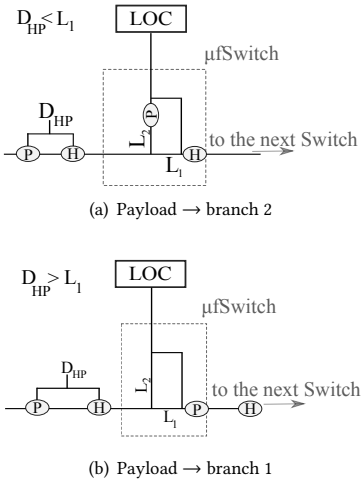

Figure 1: Switching by distance principle

by distance (DbD) switching or in the size of the header droplet [12], so-called *droplet by size (DbS)* switching.

This work complements the work in [5] and [12] by the following contributions: (i) we deliver a unified analysis of both DbD and DbS switching principles; (ii) for the first time, we derive the maximum size of a microfluidic network, i.e. the maximum number of supported LoCs, as critical parameter for the parallel processing capabilities of microfluidic networks; (iii) we define achievable throughput for DbD and DbS networks as a crucial factor for high throughput applications that screen large amounts of samples; (iv) we identify the limiting parameters for both network size and throughput; (v) we provide application based design guidelines.

2 DROPLET BY DISTANCE SWITCHING

2.1 Principle

The principle of droplet by distance switching was, for the first time, introduced in [9]. In the following we briefly review the main principle[1]: Fig. 1 shows a μfSwitch which consists of two asymmetric branches 1 and 2 of length L_1 and L_2, $L_1 < L_2$, and a bypass channel. Due to the bypass channel the switching behavior depends only on the branches 1 and 2 [4]. The hydrodynamic resistance for a rectangular channel of length L, width w, height h can be calculated as [8]

$$R = \frac{12\mu L}{h^3 w(1 - 0.63h/w)}, \tag{1}$$

where μ denotes the dynamic viscosity of the fluid in the channel. Since $L_1 < L_2$, branch 1 offers a lower hydrodynamic resistance to the flow than branch 2, i.e. $R_{L_1} < R_{L_2}$. As shown in Fig. 1, the droplets are sent in microfluidic frames, which include one payload and one header droplet of the same size. The path of the payload droplet at the μfSwitch depends on the distance D_{HP} between the payload and header droplet. Since $R_{L_1} < R_{L_2}$ the header droplet always flows into branch 1. If $D_{\mathrm{HP}} < L_1$ (cf. Fig. 1(a)), the header droplet is still in branch 1, when the payload droplet arrives at the bifurcation, and, thus it flows into branch 2. This is because the droplet in branch 1 increases the hydrodynamic resistance so that $R_{L_1} + R_{L_D} > R_{L_2}$, where R_{D} denotes the resistance increase due to the droplet. If $D_{\mathrm{HP}} > L_1$ (cf. Fig. 1(b)) the header droplet has already left branch 1 and, thus, the payload droplets flows into branch 1.

[1]Please refer to [9] for more details.

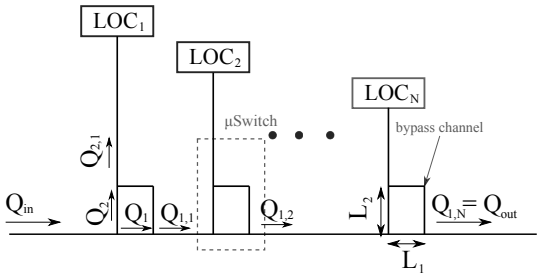

Figure 2: Bus network with DbD switching

In the following, we consider a microfluidic bus network which consists of a cascade of μfSwitches, each connected to a LoC device (cf. Fig. 2). We investigate the maximum number of supported LoCs and the achievable throughput using the DbD switching principle. For all investigations, we assume that the hydrodynamic resistance of the channel connecting the LoC to the μfSwitch is designed such that the flow rates Q_1 and Q_2 are equal to the flow rates $Q_{1,1}$ and $Q_{2,1}$, respectively (cf. Fig. 2).

2.2 Maximum Network Size

For the microfluidic bus network shown in Fig. 2 the flow rate after the first switch is given by

$$Q_{1,1} = Q_{\mathrm{in}} \frac{R_2}{R_1 + R_2} = Q_{\mathrm{in}} \frac{L_2}{L_1 + L_2}, \tag{2}$$

where R denotes hydrodynamic resistance given in (1). Moreover, we assume constant channel height, h, width, w and viscosity, μ, and, thus, $\mathrm{R} \propto L$. The flow rate after the nth switch can be derived by recursively substituting (2), resulting in

$$Q_{1,n} = Q_{\mathrm{in}} \left(\frac{L_2}{L_1 + L_2} \right)^n, \quad n = 1, \ldots, N. \tag{3}$$

In order to achieve a certain output flow rate Q_{out}, i.e. flow rate after the last switch, the maximum number of supported LoCs is given by

$$N \leq \left\lfloor \frac{\log(Q_{\mathrm{out}}/Q_{\mathrm{in}})}{\log(L_2/(L_1 + L_2))} \right\rfloor, \tag{4}$$

where $\lfloor \cdot \rfloor$ denotes the mapping to the next smaller integer number. The flow rate after each switch should be as high as possible, in ideal case close to the input flow rate Q_{in}. We notice from (3) that this can be realized through $\mathrm{L}_1 << \mathrm{L}_2$. This ensures a high flow rate along the main bus and, thus, results in a high number of supplied LoCs. However, although high values of L_2 are preferable to maximize the number of connected LoCs, it is important to note that L_2 can only be increased up to a certain value in order to satisfy the switching principle. The limits for L_2 can be expressed as follows [8]

$$0 < L_2 - L_1 < L_{\mathrm{D}} \left(\frac{\mu_d}{\mu_c} - 1 \right), \tag{5}$$

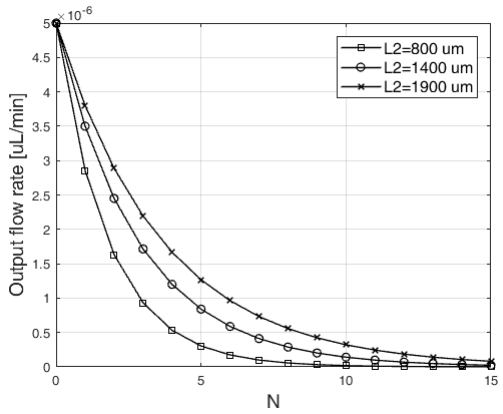

Figure 3: Output flow rate versus number of connected LoCs (N) with $L_1 = 600\,\mu$m and $L_D = 200\,\mu$m, w = $100\,\mu$m, $Q_{in} = 5\,\mu$L/min, $\mu_d/\mu_c = 9$

where $L_D = w(1 + Q_d/Q_c)$ denotes the droplet length and Q_d and $Q_c = Q_{in}$ correspond to the input flow rates for the droplet generation.

Fig. 3 shows the change of the output flow rate along the main bus for a different number of connected LoCs (N) and different values of L_2, satisfying (5). We observe that the output flow rate is decreasing more rapidly for smaller values of L_2. As expected, higher output flow rates are achieved for higher values of L_2, which ensures that more LoCs can be supplied. For example, setting the threshold output flow rate to $Q_{out} = 1.5\,\mu$L/min, a microfluidic network with switches with $L_2 = 800\,\mu$m can supply only two LoCs, whereas switches with $L_2 = 1900\,\mu$m are able to supply four LoCs.

2.3 Throughput

We determine the throughput for the worst case scenario, where all payload droplets are routed to the last LoC in the network[2]. According to (3), this gives the minimum throughput of the network, since the flow rates at the Nth switch are at minimum. We define the throughput R_{DbD} as the number of payload droplets that are successfully delivered to the Nth LoC, which can be expressed as

$$r_{DbD} = \frac{1}{t_{PP}} = \frac{v_{2,N}}{D_{PP}{}^{(N)}}, \tag{6}$$

where t_{PP} and $D_{PP}{}^{(N)}$ denotes the time and distance between two successive payload droplets traveling towards the Nth LoC, respectively. Moreover, $v_{2,N}$ corresponds to the velocity of the payload droplet moving towards the Nth LoC. As shown in Fig. 4, the distance between the payload droplets is reduced when traversing through the μfSwitches. This occurs due to the loss in the flow rate at each switch (cf. (3)). The distance reduction at the Nth switch can be expressed as follows [5]

$$D_{PP}{}^{(N)} = \frac{v_{2,N}}{v_{in}} D_{PP}{}^{(\min)}, \tag{7}$$

[2] A similar throughput was also investigated in [5], but without providing mathematical expressions.

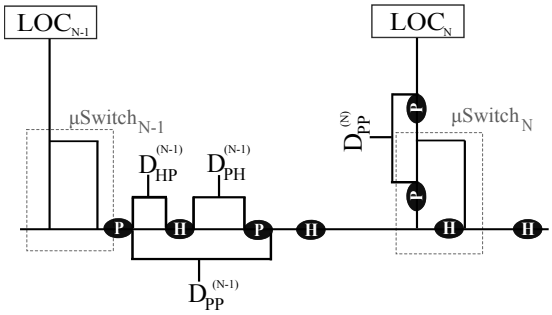

Figure 4: Droplet distances within/between microfluidic frames

where $D_{PP}{}^{(\min)}$ corresponds to the minimal achievable distance between two successive payload droplets at network input and v_{in} denotes the velocity at the network input. The velocity v_{in} is given by

$$v_{in} = \frac{Q_{in}}{A}, \tag{8}$$

where $A = wh$ denotes the cross section of the channel and Q_{in} corresponds to the flow rate at the network input. Combining (6), (7) and (8) gives the worst case throughput for a microfluidic bus network with DbD switching

$$r_{DbD} = \frac{1}{t_{PP}} = \frac{v_{in}}{D_{PP}{}^{(\min)}} = \frac{Q_{in}}{A\,D_{PP}{}^{(\min)}}. \tag{9}$$

We notice from (9) that the throughput increases as Q_{in} increases. However, it is important to note that for a correct functionality of the switching principle the input flow rate, Q_{in}, is limited by [2]

$$Q_{in} < \frac{\sigma}{\mu_c}\left(\frac{\chi w}{L_D}\right)^{\frac{1}{0.21}}, \tag{10}$$

with $\chi = 0.187$ and σ denotes the interfacial tension coefficient. The minimum distance between two payload droplets at the network input can be expressed as

$$D_{PP}{}^{(\min)} = D_{HP}{}^{(\min)} + D_{PH}{}^{(\min)} + 2L_D, \tag{11}$$

where $D_{HP}{}^{(\min)}$ and $D_{PH}{}^{(\min)}$ denote the minimum distance between header and payload droplet within one microfluidic frame and between two successive microfluidic frames (cf. Fig. 4), respectively. The minimum value for the distance between header and payload within one frame is given by [5]

$$D_{HP}{}^{(\min)} \geq C\frac{L_2}{L_1^2}\frac{v_{in}}{v_{1,N}} = C\frac{L_2}{L_1^2}\frac{1}{\left(\frac{L_2}{L_1+L_2}\right)^N}, \tag{12}$$

with $C = L_1(L_1 + L_2 + L_D(\mu_c - \mu_d))$. The minimum value for the distance between header and payload between two successive frame can be expressed as [5]

$$D_{PH}{}^{(\min)} = CL_2\frac{v_{in}}{v_{1,N-1}} = CL_2\frac{1}{\left(\frac{L_2}{L_1+L_2}\right)^{N-1}} \tag{13}$$

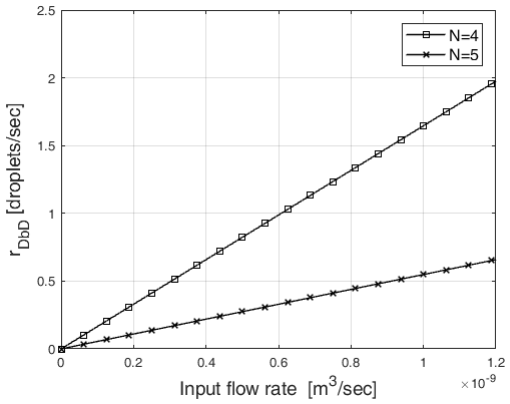

Figure 5: Throughput versus input flow rate for $L_1 = 600\,\mu$m, $L_2 = 1200\,\mu$m and $L_D = 200\,\mu$m

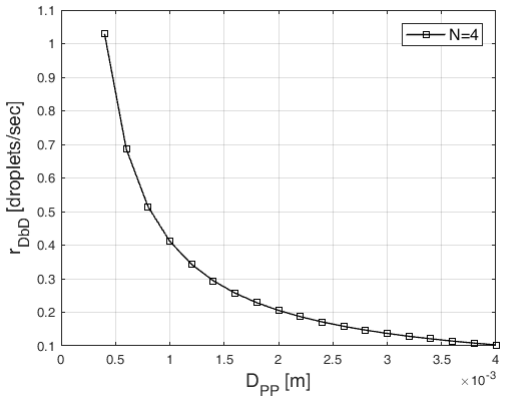

Figure 6: Throughput versus payload droplet distance for $L_1 = 600\,\mu$m, $L_2 = 1200\,\mu$m and $L_D = 200\,\mu$m

Substituting (12) and (13) into (11) results in the minimum distance between two payload droplets at the network input

$$D_{\mathrm{PP}}{}^{(\min)} \geq CL_2\left(\frac{1}{L_1^2\left(\frac{L_2}{L_1+L_2}\right)^N}+\frac{1}{\left(\frac{L_2}{L_1+L_2}\right)^{N-1}}\right)+2L_{\mathrm{D}}. \quad (14)$$

Figs. 5 and 6 show dependence of the throughput on different parameters. Fig. 5 presents the throughput r_{DbD} versus the input flow rate, Q_{in}, considering only values for Q_{in} satisfying (10). As expected, the throughput increases as the input flow rate increases (cf. (9)). Moreover, the throughput decreases as the number of connected LoCs increases. This is because, the velocity of the droplets decreases after each switch, and, thus the velocity at the last switch is the smaller the more LoCs are connected.

Fig. 6 shows the throughput r_{DbD} versus the payload droplet distance $D_{\mathrm{PP}} \geq D_{\mathrm{PP}}{}^{(\min)}$. As expected, the throughput decreases as D_{PP} increases (cf. (9)). The maximum throughput is achieved for $D_{\mathrm{PP}} = D_{\mathrm{PP}}{}^{(\min)}$. Using (14) we obtain $D_{\mathrm{PP}}{}^{(\min)} = 0.45\,$mm, with $N = 4$, $L_2/L_1 = 2$, and $L_{\mathrm{D}} = 200\,\mu$m. This results in a throughput of $r_{\mathrm{DbD}} = 1\,$droplets$/s$ which can be confirmed by Fig. 6.

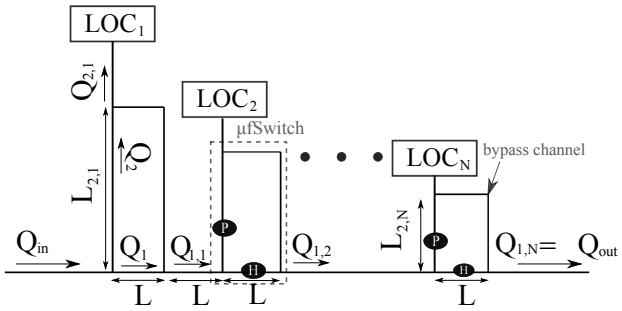

Figure 7: Bus network with μfSwitch for DbS switching

3 DROPLET BY SIZE SWITCHING

3.1 Principle

The droplet by size switching principle was introduced in [1, 12]. In contrast to DbD switching, the path of the payload droplet at the μfSwitch is determined by the size of the header droplet, while the distance between header and payload droplet is fixed. Moreover, microfluidic networks with DbS switching mechanism have an exclusive network access policy, i.e. a new pair of payload-header droplets can only be injected once the previous pair has left the network. Hence, at all times, only one payload-header droplet pair can be within the network[3].

In the following, we complement the work in [1, 12] by delivering a mathematical model on how the geometry between successive μfSwitches changes depending on the number of connected LoCs. Similar to Sec. 2, we investigate the maximum number of connected LoCs and the achievable throughput using the DbS switching principle and determine limiting parameters for both metrics. Moreover, we assume that the flow rates Q_1 and Q_2 are equal to the flow rates $Q_{1,1}$ and $Q_{2,1}$, respectively (cf. Fig. 7).

3.2 Maximum Network Size

Similar to Sec. 2, we consider a microfluidic bus network as shown in Fig. 7, including μfSwitches with two asymmetric branches 1 and 2 of lengths $L_{1,n}$ and $L_{2,n}$, with $L_{1,n} < L_{2,n}\ \forall n$. However, in contrast to Sec. 2, the asymmetry between the branches is reduced when moving from the first to the last μfSwitch. Similar to (3), the flow rate after the nth switch can be calculated as

$$Q_{1,n} = Q_{\mathrm{in}}\prod_{i=1}^{n}\frac{R_{2,i}}{R+R_{2,i}} = Q_{\mathrm{in}}\prod_{i=1}^{n}\frac{L_{2,i}}{L+L_{2,i}}, \quad n = 1,\ldots,N. \quad (15)$$

where $L_{2,i}$ is decreasing as the number of connected LoCs is increasing, i.e., $L_{2,1} > L_{2,2} \ldots > L_{2,N}$, and $L_{1,n} = L$. In order to guarantee the correct functionality of the switching principle, the geometry of the μfSwitches need to satisfy the following conditions [1]

$$L_{2,n} - L < \frac{w}{\alpha}\rho_n < L_{2,n-1} - L \quad (16)$$

$$L_{1,n} < L_{2,n}, \quad (17)$$

for $n = 1,\ldots,N$. The resistance increment induced due to the droplet injected into the channel is denoted by ρ_n and $\alpha = (12\mu)/(h^3(1-0.63h/w)$. After some mathematical manipulations, not shown here

[3]Please refer to [1, 12] for a detailed discussion on the switching principle.

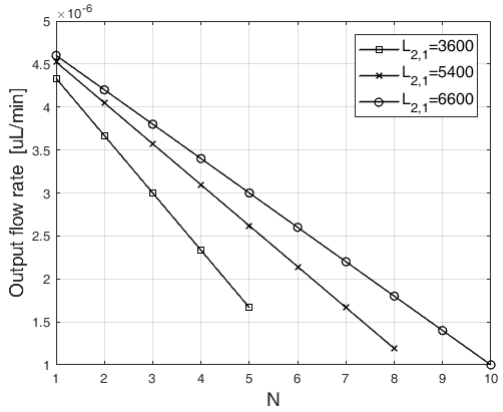

Figure 8: Output flow rate after every switch for $L_1 = 600\,\mu$m

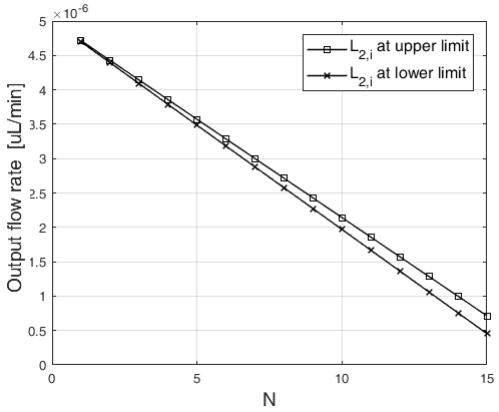

Figure 9: Output flow rate versus number of connected LoCs (N) for upper and lower limits of $L_{2,i}$ with N = 15, $L_1 = 600\,\mu$m and $\beta = 0.5$

due to the lack of space, we obtain the following range for the length of branch 2

$$L_{2,n} - L < L(N - (n-1) + \beta) < L_{2,n-1} - L. \tag{18}$$

According to (18), the maximum number of connected LoCs is limited by the degree of freedom available in choosing $L_{2,N}$, while satisfying the switching limitations from (17). Hence, in order to define N we first define geometrical limitations for $L_{2,N}$. From (18) we derive an upper and a lower limit for $L_{2,N}$. Using $n = N + 1$ in (18) results in the lower limit

$$L_{2,N} > L(\beta + 1). \tag{19}$$

The upper limit is obtained by applying $n = N$ in (18)

$$L_{2,N} < L(\beta + 2). \tag{20}$$

Using (18) – (20) we can derive the maximum number of supported LoC which is given by

$$N \leq \left\lfloor \frac{L_{2,1} - 2L}{L} + 1 \right\rfloor. \tag{21}$$

In principle, more LoCs can be added to the DbS network as long as the length of branch 2 of the newly added μfSwitch, satisfies (17) and (18). Fig. 8 shows the change of the output flow rate of every switch (cf. (15)) for different values of $L_{2,1}$. We observe that with larger values of the branch length $L_{2,1}$ more LoCs can be supported. Once all geometries in the network are known and N is derived, it can be verified how many LoCs can be supplied at minimum with a certain output flow rate. For example, $Q_{\text{out}} = 1.5\,\mu$L/min, a microfluidic network with $L_{2,1} = 3600\,\mu$m can support up to five LoCs, but with $L_{2,1} = 6600\,\mu$m only up to eight LoCs can be supplied (cf. (21)).
Since (18) only gives a range of acceptable values for the lengths of branches 2 for every μfSwitch, we investigate the influence of the choice on the output flow rate. We observe from Fig. 9 that the upper range of the values is preferable for achieving higher flow rates. Moreover, the choice of the value has more affect on the output flow rate as the number of connected LoCs increases.

3.3 Throughput

Similar to Sec. 2.3 we determine the worst-case throughput, assuming that all payload droplets are routed to the last LoC in the network. Due to the limitation of having only one droplet pair at the time in the network (exclusive network policy), we derive time needed for droplet pair to leave the network through Nth LoC. We assume that the channel at the input, i.e. before the first switch, has length $2L$ and that we collect the output of the network immediately at the point after the last switch. In this case, the distances that payload and header droplets travel are are given by

$$D_{\text{P}} = 2L(N + 1), \tag{22}$$

$$D_{\text{H}} = L(2N + 1). \tag{23}$$

We notice from (22) and (23) that the payload droplet needs to travel a larger distance to exit the network than header droplet. Hence, the time for the payload droplet to leave the system is the limiting parameter for evaluating the throughput. We define the time needed for payload droplet to travel from the input to the Nth LoC by

$$t_{\text{P}} = \frac{1}{r_{\text{DbS}}} = \frac{D_{\text{P}}}{v} = \frac{2L(N+1)}{v} = \frac{2L}{v_{in} + \sum_{i=1}^{N-1} v_{1,i} + v_{2,N}} \tag{24}$$

Using the relation $v = Q/A$ and applying (2), (24) can be written as

$$t_{\text{P}} = \frac{2LA}{Q_{\text{in}}\left(1 + \sum_{i=1}^{N-1}\prod_{j=1}^{i}\frac{L_{2,j}}{L + L_{2,j}} + \frac{L}{L + L_{2,N}}\prod_{j=1}^{N-1}\frac{L_{2,j}}{L + L_{2,j}}\right)}. \tag{25}$$

Thus, the throughput for a microfluidic bus network with DbS switching is given by

$$r_{\text{DbS}} = \frac{Q_{\text{in}}\left(1 + \sum_{i=1}^{N-1}\prod_{j=1}^{i}\frac{L_{2,j}}{L + L_{2,j}} + \frac{L}{L + L_{2,N}}\prod_{j=1}^{N-1}\frac{L_{2,j}}{L + L_{2,j}}\right)}{2LA}. \tag{26}$$

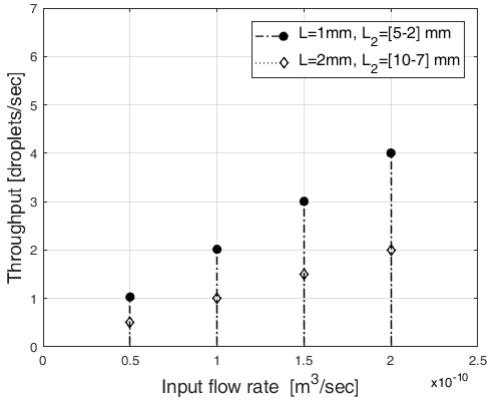

Figure 10: Throughput versus input flow rate for N = 4 and different values of L and L_2. In the range for L_2 the highest value is shown at the left

We notice from (26) that the throughput depends on many different parameter like input flow rate Q_{in}, branch lengths of the μfSwitches $L_{1,n} = L$ and $L_{2,n}$, the channel cross-section A and the number of connected LoCs, N. Moreover, it is important to not that the exclusive access policy harms the throughput of the network. Fig. 10 shows the dependence of the throughput on different parameters. We observe that the throughput increases as the input flow rate increases. Moreover, a higher throughput is achieved if the branch lengths L and L_2 are small.

4 COMPARISON OF DBD AND DBS

In this section, we provide a comparative summary of the obtained results, together with application-based design guidelines. The typical design process for a microfluidic device starts by defining geometrical constraints, usually imposed by a specific application and/or fabrication process. In order to make a fair comparison between DbD and DbS networks, we assume the same design constraints for both networks. We limit the branch lengths of the μfSwitch to a range between 600 μm and 4000 μm. Moreover, we assume a constant height and width of all channels in the network, with $w = 150\,\mu$m and $h = 50\,\mu$m.

From Fig. 3 ($L_2 = 1900\,\mu$m) and Fig. 8 ($L_{2,1} = 3600\,\mu$m) we observe that DbD microfluidic networks can support more LoCs, up to fifteen, compared to DbS networks, at most five. Interestingly, the output flow rate is the main limiting parameter for the network size. In this regard, in applications where higher output flow rates are required, DbS network can support more LoCs than DbD network. From Figs. 5 and 10 we notice that throughput is increasing with increasing input flow rate. However, to achieve the same throughput, DbD network requires much higher input flow rates than DbS network. For example, to achieve a throughput of $r = 2$ droplets/s in a network with $N = 4$ LoCs, a DbD network requires an input flow rate of $Q_{\text{in}} = 1.2\,\text{nm}^3/\text{s}$ while a DbS network achieves same throughput with a flow rate of $Q_{\text{in}} = 0.1\,\text{nm}^3/\text{s}$. Additionally, we notice from from Fig. 10 that reducing the length of branch 2 increases the throughput for DbS networks. However, in DbS networks throughput suffers from exclusive network access policy, which limits the network to hold only single pair of droplets at the time. This is in contrast to DbD networks where the network can hold multiple droplet pairs at the same time. For this reason, applications where parallelism is of an importance, DbD network can offer better performance.

For applications where simplicity in the design and geometrical structure of networks are important, DbD networks are of advantage due to their simple structure and generic switch design. In DbD netoworks, all μfSwitches have same geometrical characteristics and all droplets are of same size. This is in contrast to DbS networks where every switch has different geometry and droplets of various sizes are used.

5 CONCLUSION

In this paper, two concepts of passive droplet routing in microfluidic bus networks have been analyzed and compared: Droplet by distance (DbD) switching and droplet by size (DbS) switching. In particular, the focus has been on deriving the maximum network size and achievable throughput, as two crucial metrics for the applicability of these networks in modern microfluidic applications. Additionally, we have identified limiting parameters for both metrics and provided design guidelines according to these limitations. Assuming the same design constraints we have compared both approaches and made the following observation: DbD networks can support larger network sizes, offer multiple network access policy and simpler design, but suffer from lower throughput. On the other hand DbS networks, achieve a higher throughput, but the design is more complex and the maximum network size is smaller.

REFERENCES

[1] A. Biral and A. Zanella. 2013. Introducing purely hydrodynamic networking mechanisms in microfluidic systems. In *Proc. Int. Conf. Communications*. 798 – 803.
[2] A. Biral, D. Zordan, and A. Zanella. 2015. Modeling, Simulation and Experimentation of Droplet-Based Microfluidic Networks. *IEEE Trans. Mol. Biol. Multi-Scale Commun.* 1, 2 (June 2015), 122 – 134.
[3] G. Castorina, M. Reno, L. Galluccio, and A. Lombardo. 2017. Microfluidic networking: Switching multidroplet frames to improve signaling overhead. *Nano Commun. Netw.* 14 (Dec. 2017), 48 – 59.
[4] G. Cristobal, J.-P. Benoit, M. Joanicot, and A. Ajdari. 2006. Microfluidic bypass for efficient passive regulation of droplet traffic at a junction. *Appl. Phys. Lett.* 89, 3 (July 2006), 034104–1 – 034104–3.
[5] L. Donvito, L. Galluccio, A. Lombardo, and G. Morabito. 2016. μ-NET: A Network for Molecular Biology Applications in Microfluidic Chips. *IEEE/ACM Trans. Netw.* 24, 4 (Aug. 2016), 2525 – 2538.
[6] A. Grimmer, W. Haselmayr, A. Springer, and R. Wille. 2017. A Discrete Model for Networked Labs-on-Chips: Linking the Physical World to Design Automation. In *Proc. Design Automation Conf.* 50:1 – 50:6.
[7] A. Grimmer, W. Haselmayr, A. Springer, and R. Wille. 2018. Design of Application-specific Architectures for Networked Labs-on-Chips. *IEEE Trans. Comput.-Aided Design Integr. Circuits Syst.* 37, 1 (Jan. 2018), 193 – 202.
[8] E. De Leo, L. Donvito, L. Galluccio, A. Lombardo, G. Morabito, and L. M. Zanoli. 2013. Communications and Switching in Microfluidic Systems: Pure Hydrodynamic Control for Networking Labs-on-a-Chip. *IEEE Trans. Commun.* 61, 11 (Nov. 2013), 4663 – 4677.
[9] E. De Leo, L. Galluccio, A. Lombardo, and G. Morabito. 2012. Networked labs-on-a-chip (NLoC): Introducing Networking Technologies in Microfluidic Systems. *Nano Commun. Netw.* 3, 4 (Dec. 2012), 217 – 228.
[10] D. Mark, S. Haeberle, G. Roth, F. von Stetten, and R. Zengerle. 2010. Microfluidic lab-on-a-chip platforms: Requirements, characteristics and applications. *Chemical Society Reviews* 39, 3 (2010), 1153 – 1182.
[11] S.-Y. Teh, R. Lin, L.-H. Hung, and A. P. Lee. 2008. Droplet microfluidics. *Lab on a Chip* 8 (2008), 198 – 220. Issue 2.
[12] A. Zanella and A. Biral. 2014. Design and analysis of a microfluidic bus network with bypass channels. In *Proc. Int. Conf. Communications*. 3993 – 3998.